Analytical evaluation of short-range forces in cylindrical geometry

1996 J. Phys. A: Math. Gen. 29 4649

(http://iopscience.iop.org/0305-4470/29/15/030)

J. Phys. A: Math. Gen. **29** (1996) 4649–4663. Printed in the UK

Analytical evaluation of short-range forces in cylindrical geometry

N A Lockerbie, A V Veryaskin and X Xu

Department of Physics and Applied Physics, Strathclyde University, 107 Rottenrow, Glasgow G4 0NG, UK

Received 31 July 1995, in final form 26 January 1996

Abstract. This paper concerns the potential field for Yukawa-type forces in a cylindrical geometry. A set of formulae is derived for a cylindrical body in order to reduce the integration over the body from 3D (or 6D for a pair of interacting bodies) to either a 1D integration, or an analytical formula. Using these formulae we consider analytically the potential field of two Yukawa force terms, and reanalyse Long's and Spero *et al*'s experiments for the inverse-square law test. The results show that the α–λ graph produces similar results to the case where a single Yukawa term is considered. The theory can also be applied to other problems in short-range force experiments that involve cylindrically shaped bodies as the test masses.

1. Introduction

During the last twenty years the intriguing possibility has arisen of the existence of a weak gauge force coming from different theoretical schemes in particle physics. On the macroscale it could lead to a violation of the classical Newtonian inverse square law of gravitation. However, the inverse square law is known to agree with astronomical data to very high accuracy, and has been widely accepted for the gravitational field at these distances. Furthermore, the inverse square law has been confirmed for the distance range from 1 km to several astronomical units. However, it is currently under experimental investigation at shorter distances.

The interest in such experiments comes mainly from the theoretical effort of unifying gravity with the other three forces of Nature, as this would result in the gravitational force being mediated by an exchange of particles. In some models various massless particles would lead to a Yukawa-like contribution to the gravitational interaction potential between massive bodies. Such forces are 'long-range', and can be observed—in principle—on the laboratory scale of length. Deviations from the inverse square law can arise in two ways: as a true departure of gravity itself, or through additional non-gravitational forces. In the first case the deviation would be the same for all materials; but if instead there were additional forces that could become confused with gravity, then their effects might depend upon the nature of the material. In the first case above, the gravitational potential would have the form $-(GM/r)(1+\alpha e^{-r/\lambda})$, and one of the aims of recent gravitational experiments in the laboratory has been to set limits to such deviations from the inverse square law.

Historically, the first laboratory experiment on the inverse square law was carried out by Mackenzie, in 1895. He used a torsion balance and obtained the result that the inverse square law was valid to about 1% at distances of 30 to 70 mm (at the limit of experimental error). Following this, no further experiments of this type were made until that of Long (1976).

0305-4470/96/154649+15$19.50

Long used a torsion balance with two ring masses, one large and one small. He placed in turn attracting masses in the form of the two rings opposite a test mass on one end of the beam of a torsion balance. At that distance the Newtonian forces from the two rings should have been equal. His result was expressed in terms of the relative difference of torque produced by the two rings. If interpreted in terms of the parameter $\alpha\mu^2(\mu = 1/\lambda)$, then his result was $0.07 < \alpha\mu^2 < 0.1$ at a distance of from 0.025 to 0.175 (m). If $\alpha = \frac{1}{3}$, for example, then λ lies between 1.8 and 2.2 m. This was the result that was analysed by Chen (1982), using his non-Newtonian formulae.

Spero *et al* (1980) carried out an experiment analogous to the Faraday cage in electromagnetism. The Newtonian force inside a long (apparently infinitely long) cylinder is zero, whilst a non-Newtonian force is not, and should be proportional to the product of α and μ^2. The principle of the experiment was to look for deflections of the balance as the cylinder was moved from side to side while the test mass was fixed in the initial centre of the cylinder. However, their experimental result interpreted by Chen (1982) was quite different from Long's. In terms of the $\alpha\mu^2(\mu = 1/\lambda)$ parameter, $\alpha\mu^2 < 0.029\ \mathrm{m}^{-2}$ i.e. if $\alpha = 1/3$ then $\lambda > 3.4$ m.

Chen and Cook *et al* in Cambridge (1984) subsequently carried out two groups of experiments, prompted by the different results of Long and Spero *et al*. In the one group the net force on the test mass was made close to zero, while in the other there was a net force. They used three cylindrical masses, and measured the torque difference due to the different masses—comparing their results with their theoretical predictions. Their non-null result was $\lambda > 3.4$ m for $\alpha = \frac{1}{3}$, whilst their null result was $\lambda > 4.9$ m for the same value of α. Therefore, Chen *et al*'s results are consistent with those of Spero *et al*.

Others have also carried out gravitational experiments to test the inverse square law, most of their experimental results being in conflict with Long's positive result. This can be seen clearly from the α–λ graph of figure 1. However, it is still unknown why Long's result was different from that of other workers. From the interpretational point of view, the method used by Chen assumes that the ring is an ideal one without thickness. Thus his analytical formulae are only approximations. It is therefore worthwhile to reanalyse these experiments using a full analytical formula which treats the masses as true 3D bodies.

As in other kinds of gravitational experiments (such as the measurement of the constant of gravitation, G), the torsion balance is still the main detector used in the laboratory to verify the inverse square law, and the cylindrical body once again is the most often used form for the attracting mass. If the interaction between the attracting mass and test mass is not an inverse square relationship, then classical formulae developed for the potentials and attractions of Newtonian gravity will not be applicable. Therefore, formulae for non-Newtonian forces in different situations will need to be developed, because even a perfect sphere cannot then be treated as a point mass.

There are two effects of non-Newtonian forces in laboratory experiments, one coming from the physical separation of the attracting mass from the attracted mass, and the other arising from the geometric shapes of the masses themselves. In this work, some examples of analytic solutions to non-Newtonian force problems will be presented for the case of cylindrical geometry, since, as mentioned above, most test masses in gravitational experiments use such cylindrically shaped bodies. These solutions will be used below to reanalyse the Long and Spero *et al* experiments; but they have wider applicability in the interpretation and design of other experiments in the search for the existence of non-Newtonian forces.

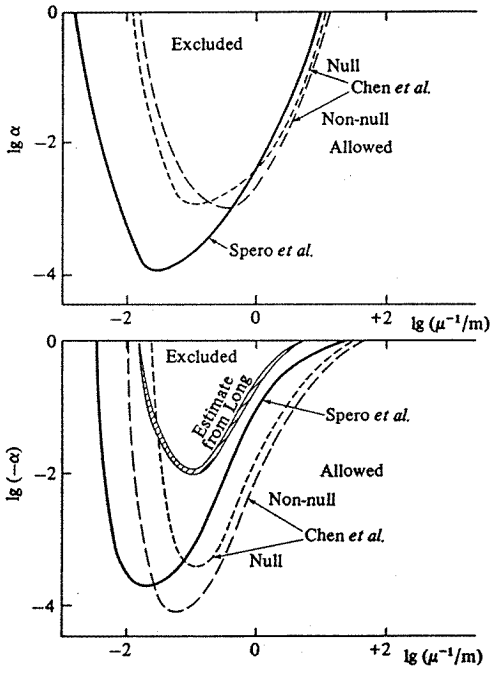

Figure 1. Allowed values of the Yukawa 'strength' and 'range' parameters α and λ. Upper figure: $\alpha > 0$; lower figure: $\alpha < 0$. The regions bounded by the curves and the $|\alpha| = 1$ line are excluded, i.e. the inverse square law is followed.

2. The potential of a Yukawa-type force in the cylindrical coordinate system

The potential V_λ of a non-Newtonian force (for example a Yukawa-type force), due to a distribution of mass of density ρ, obeys the modified Helmholtz equation

$$\nabla^2 V_\lambda - \frac{1}{\lambda^2} V_\lambda = 4\pi G\alpha\rho(\boldsymbol{R}) \tag{1}$$

where λ is the scale of the force action, and α is the coupling constant. The sign of α can be either positive or negative, in other words the overall attractive force may yet have a repulsive component. The solution of equation (1) is well known to be

$$V_\lambda(\boldsymbol{R}) = -G\alpha \int_{\tau'} \frac{\rho(\boldsymbol{R}')}{|\boldsymbol{R} - \boldsymbol{R}'|} \mathrm{e}^{-|\boldsymbol{R}-\boldsymbol{R}'|/\lambda}\, \mathrm{d}\tau' \tag{2}$$

where the primed integration is carried out over the volume of the body of mass density $\rho(\boldsymbol{R}')$, the general point is labelled $\boldsymbol{R} \equiv (r, \varphi, z)$, and a point within the body is labelled $\boldsymbol{R}' \equiv (r', \varphi', z')$, as shown in figure 2.

For the Newtonian force we know that the gravitational potential due to a distribution of mass of density ρ is

$$V(\boldsymbol{R}) = -G \int_{\tau'} \frac{\rho(\boldsymbol{R}')}{|\boldsymbol{R} - \boldsymbol{R}'|}\, \mathrm{d}\tau \tag{3}$$

and the Green's function can be written as (Lockerbie *et al* 1993)

$$\frac{1}{|\boldsymbol{R} - \boldsymbol{R}'|} = \sum_{m=0}^{\infty} \varepsilon_m \cos m(\varphi - \varphi') \int_0^\infty \mathrm{d}k J_m(kr) J_m(kr') \mathrm{e}^{-k|z-z'|} \tag{4}$$
$$\varepsilon_m = 1 \ (m = 0) \qquad \varepsilon_m = 2 \ (m > 0)$$

where the $J_m(x)$ are the ordinary Bessel functions of order m.

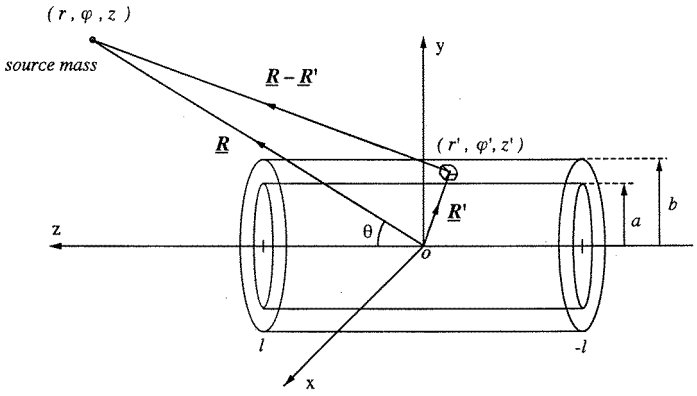

Figure 2. The geometry used for the calculation of the non-Newtonian interaction between a unit source mass and a hollow cylindrical body.

In the following we will show that the function $\frac{e^{-|R-R'|/\lambda}}{|R-R'|}$ may be written as

$$\frac{e^{-|R-R'|/\lambda}}{|R-R'|} = \sum_{n=0}^{\infty} \varepsilon_n \cos n(\varphi-\varphi') \int_0^{\infty} \frac{1}{\sqrt{k^2+1/\lambda^2}}\, dk\, k J_n(kr) J_n(kr') e^{-\sqrt{k^2+1/\lambda^2}|z-z'|} \tag{5}$$

$\varepsilon_n = 1\ (n=0) \qquad \varepsilon_n = 2\ (n>0).$

Using this formula the interesting cases of (i) the non-Newtonian interaction between 'source' and 'test' masses in the form of cylindrical bodies, and (ii) some important experiments for testing the inverse square law, will be analysed.

First of all a set of functions

$$f_{s,k,n}(\boldsymbol{R}) = \frac{\sqrt{k}}{2\pi} J_n(kr) e^{in\varphi + isz} \tag{6}$$

will be defined, where $0 \leqslant k \leqslant \infty$, $-\infty \leqslant s \leqslant \infty$, $n = 0, \pm 1, \pm 2, \ldots$.

It is straightforward to show that the set of functions are orthonormal in a whole space, so that

$$\int_0^{2\pi} d\varphi \int_{-\infty}^{\infty} dz \int_0^{\infty} f_{s,k,n}(\boldsymbol{R}) f^*_{s',k',n'}(\boldsymbol{R}) r\, dr = \delta_{nn'}\delta(s-s')\delta(k-k') \tag{7}$$

where the superscript $*$ denotes complex conjugation, $\delta_{nn'}$ is the Kronneker delta, and $\delta(x)$ is the Dirac delta-function†.

The functions in (6) are the eigenfunctions of the 3-dimensional modified Helmholtz equation in the cylindrical coordinate system

$$\nabla^2 f + (s^2 + k^2) f = 0. \tag{8}$$

This is so because the modified Helmholtz equation can be expressed in circular cylindrical coordinates (r, φ, z) as

$$\frac{1}{r}\frac{\partial}{\partial r}\left(r\frac{\partial f}{\partial r}\right) + \frac{1}{r^2}\frac{\partial^2 f}{\partial \varphi^2} + \frac{\partial^2 f}{\partial z^2} + (s^2+k^2) f = 0$$

† Let $\boldsymbol{Q} \equiv (s, k, n)$ be a vector in the index manifold, and let $\int d\boldsymbol{Q} \equiv \sum_{n=-\infty}^{\infty} \int_{-\infty}^{\infty} ds \int_0^{\infty} dk$. Then the functions $f_Q(\boldsymbol{R})$ defined in (6) represent an *orthonormal and complete* set of functions on R^3, since for any quadratically integrable function $P(\boldsymbol{R})$ we have, (i) $P(\boldsymbol{R}) = \int d\boldsymbol{Q} \cdot p_Q \cdot f_Q(\boldsymbol{R})$, and (ii) $\int P^2(\boldsymbol{R}) \cdot d\boldsymbol{R} = \int d\boldsymbol{Q} \cdot p_Q^2$ (the Parseval, or completeness, identity).

and the general solution to this equation can be written in separable form $f = \Phi(\varphi)\Re(r)Z(z)$, where $\Re$, Φ, and Z are solutions of the separated equations

$$\frac{1}{r}\frac{\mathrm{d}}{\mathrm{d}r}\left(r\frac{\mathrm{d}\Re}{\mathrm{d}r}\right) + \left(k^2 - \frac{n^2}{r^2}\right)\Re = 0 \qquad \text{solutions: } \Re = J_n(kr)$$

$$\frac{\mathrm{d}^2 Z}{\mathrm{d}z^2} + s^2 Z = 0 \qquad \text{solutions: } Z = \mathrm{e}^{\mathrm{i}sz}$$

$$\frac{\mathrm{d}^2 \Phi}{\mathrm{d}\varphi^2} + n^2 \Phi = 0 \qquad \text{solutions: } \Phi = \mathrm{e}^{\mathrm{i}n\varphi}$$

so that one can write the eigenfunctions as $f_{s,k,n}(\boldsymbol{R}) = \frac{\sqrt{k}}{2\pi} J_n(kr)\mathrm{e}^{\mathrm{i}n\varphi + \mathrm{i}sz}$, as in (6) above.

Now let the Yukawa potential $V_\lambda(\boldsymbol{R})$ be

$$V_\lambda(\boldsymbol{R}) = \sum_{n=-\infty}^{\infty} \int_{-\infty}^{\infty} \mathrm{d}s \int_0^{\infty} V(s,k,n) f_{s,k,n}(\boldsymbol{R})\,\mathrm{d}k. \tag{9}$$

Thus equation (9) is simply an expansion of the potential in terms of the cylindrical eigenfunctions of modified Helmholtz equation, $\frac{\sqrt{k}}{2\pi} J_n(kr)\mathrm{e}^{\mathrm{i}n\varphi + \mathrm{i}sz}$, with discrete eigenvalues n, and two continuous eigenvalue spectra in k and s.

Substituting equation (9) into equation (1), and using equation (8), leads to

$$\sum_{n=-\infty}^{\infty} \int_{-\infty}^{\infty} \mathrm{d}s \int_0^{\infty} V(s,k,n) f_{s,k,n}(\boldsymbol{R})(-s^2 - k^2)\,\mathrm{d}k - \frac{1}{\lambda^2} V_\lambda(\boldsymbol{R}) = 4\pi G\alpha\rho(\boldsymbol{R})$$

which can be written as

$$\sum_{n=-\infty}^{\infty} \int_{-\infty}^{\infty} \mathrm{d}s \int_0^{\infty} V(s,k,n) f_{s,k,n}(\boldsymbol{R}) \left(s^2 + k^2 + \frac{1}{\lambda^2}\right) \mathrm{d}k = -4\pi G\alpha\rho(\boldsymbol{R}).$$

Multiplying by the complex conjugate $f^*_{s',k',n'}(\boldsymbol{R})$, integrating over all values of s and k, and summing over n, we have

$$\sum_{n=-\infty}^{\infty} \int_{-\infty}^{\infty} \mathrm{d}s \int_0^{\infty} V(s,k,n) \left(s^2 + k^2 + \frac{1}{\lambda^2}\right) \mathrm{d}k \int_\tau f_{s,k,n}(\boldsymbol{R}) f^*_{s',k',n'}(\boldsymbol{R})\,\mathrm{d}\tau$$
$$= -4\pi G\alpha \int_\tau f^*_{s',k',n'}(\boldsymbol{R})\rho(\boldsymbol{R})\,\mathrm{d}\tau.$$

Using equation (7), the equation above becomes

$$\sum_{n=-\infty}^{\infty} \int_{-\infty}^{\infty} \mathrm{d}s \int_0^{\infty} V(s,k,n) \left(s^2 + k^2 + \frac{1}{\lambda^2}\right) \delta_{nn'}\delta(k-k')\delta(s-s')\,\mathrm{d}k$$
$$= \left(s'^2 + k'^2 + \frac{1}{\lambda^2}\right) V(s',k',n')$$
$$= -4\pi G\alpha \int_\tau f^*_{s',k',n'}(\boldsymbol{R})\rho(\boldsymbol{R})\,\mathrm{d}\tau.$$

Now substituting $V(s,k,n) = -\frac{4\pi G\alpha}{(s^2+k^2+1/\lambda^2)} \int_{\tau'} f^*_{s,k,n}(\boldsymbol{R}')\rho(\boldsymbol{R}')\,\mathrm{d}\tau'$ into equation (9) leads to

$$V_\lambda(\boldsymbol{R}) = -4\pi G\alpha \int_{\tau'} \rho(\boldsymbol{R}')\,\mathrm{d}\tau' \left\{ \sum_{n=-\infty}^{\infty} \int_{-\infty}^{\infty} \mathrm{d}s \int_0^{\infty} \frac{f_{s,k,n}(\boldsymbol{R}) f^*_{s,k,n}(\boldsymbol{R}')}{\left(s^2 + k^2 + \frac{1}{\lambda^2}\right)}\,\mathrm{d}k \right\}. \tag{10}$$

Comparing equation (10) with equation (2) it is obvious that

$$\frac{\mathrm{e}^{-|\boldsymbol{R}-\boldsymbol{R}'|/\lambda}}{|\boldsymbol{R}-\boldsymbol{R}'|} = -4\pi \sum_{n=-\infty}^{\infty} \int_{-\infty}^{\infty} \mathrm{d}s \int_0^{\infty} \frac{f_{s,k,n}(\boldsymbol{R}) f^*_{s,k,n}(\boldsymbol{R}')}{\left(s^2+k^2+\frac{1}{\lambda^2}\right)} \,\mathrm{d}k$$
$$= -\frac{1}{\pi} \sum_{n=-\infty}^{\infty} \mathrm{e}^{\mathrm{i}n(\varphi-\varphi')} \int_0^{\infty} k J_n(kr) J_n(kr') \left\{ \int_{-\infty}^{\infty} \frac{\mathrm{e}^{\mathrm{i}s(z-z')}}{\left(s^2+k^2+\frac{1}{\lambda^2}\right)} \,\mathrm{d}s \right\} \mathrm{d}k. \quad (11)$$

The integral inside the braces in equation (11) is well known (Prudnikov *et al* 1986):

$$\int_{-\infty}^{\infty} \frac{\mathrm{e}^{\mathrm{i}s(z-z')}}{\left(s^2+k^2+\frac{1}{\lambda^2}\right)} \,\mathrm{d}s = -\frac{\pi \mathrm{e}^{-|z-z'|\sqrt{k^2+1/\lambda^2}}}{\sqrt{k^2+1/\lambda^2}}. \quad (12)$$

Substituting equation (12) into equation (11), we finally get

$$\frac{\mathrm{e}^{-|\boldsymbol{R}-\boldsymbol{R}'|/\lambda}}{|\boldsymbol{R}-\boldsymbol{R}'|} = \sum_{n=-\infty}^{\infty} \mathrm{e}^{\mathrm{i}n(\varphi-\varphi')} \int_0^{\infty} \frac{k}{\sqrt{k^2+1/\lambda^2}} J_n(kr) J_n(kr') \mathrm{e}^{-\sqrt{k^2+1/\lambda^2}|z-z'|} \,\mathrm{d}k. \quad (13)$$

Thus, the potential of a Yukawa-type force due to a distribution of mass of density ρ can be written as

$$V_\lambda(\boldsymbol{R}) = 4\pi G\alpha \int_{\tau'} \rho(\boldsymbol{R}') \,\mathrm{d}\tau' \sum_{n=0}^{\infty} \varepsilon_n \cos n(\varphi-\varphi')$$
$$\times \int_0^{\infty} \frac{k}{\sqrt{k^2+1/\lambda^2}} J_n(kr) J_n(kr') \mathrm{e}^{-\sqrt{k^2+1/\lambda^2}|z-z'|} \,\mathrm{d}k \quad (14)$$

where $\varepsilon_n = 1$, $(n = 0)$; $\varepsilon_n = 2$, $(n > 0)$.

3. The interaction of a Yukawa-type force between a unit point-mass and a finite hollow cylinder

First of all we find the potential energy of a *unit* mass at position (r, φ, z), in the potential field of equation (14), produced by a bulk hollow cylinder having a density, semi-length, and inner and outer radii denoted by ρ, ℓ, a and b, respectively. The geometry is shown in figure 2, where the origin of the coordinate system is placed at the centre of mass of the cylinder. Therefore, we have a mutual potential energy of

$$U_\lambda(r,\varphi,z) = 4\pi G\alpha\rho \sum_{n=0}^{\infty} \varepsilon_n \int_0^{2\pi} \cos n(\varphi-\varphi') \,\mathrm{d}\varphi' \int_{k=0}^{\infty} \frac{k \,\mathrm{d}k}{\sqrt{k^2+1/\lambda^2}}$$
$$\times \int_a^b J_n(kr) J_n(kr') r' \,\mathrm{d}r' \int_{-\ell}^{\ell} \mathrm{e}^{-\sqrt{k^2+1/\lambda^2}|z-z'|} \,\mathrm{d}z'. \quad (15)$$

The integration depends on the position of the mass with respect to the z axis. If $z \leqslant -\ell$ or $z \geqslant \ell$ then

$$U_\lambda(r,z) = -2\pi G\alpha\rho \int_0^{\infty} \frac{J_0(kr) \,\mathrm{d}k}{k^2+1/\lambda^2} [bJ_1(kb) - aJ_1(ka)]$$
$$\times \left[\mathrm{e}^{-\sqrt{k^2+1/\lambda^2}(z-\ell)} - \mathrm{e}^{-\sqrt{k^2+1/\lambda^2}(z+\ell)} \right] \quad (16)$$

and if $-\ell \leqslant z \leqslant \ell$ then

$$U_\lambda(r,z) = -2\pi G\alpha\rho \int_0^{\infty} \frac{J_0(kr) \,\mathrm{d}k}{k^2+1/\lambda^2} [bJ_1(kb) - aJ_1(ka)]$$
$$\times \left[2 - \mathrm{e}^{-\sqrt{k^2+1/\lambda^2}(\ell-z)} - \mathrm{e}^{-\sqrt{k^2+1/\lambda^2}(\ell+z)} \right]. \quad (17)$$

The axial force can be found from the first derivative of equation (16) or equation (17), as appropriate, and we represent these two cases in equations (18) and (19) below, for $z \leqslant -\ell$ or $z \geqslant \ell$, and $-\ell \leqslant z \leqslant \ell$, respectively.

$$F_{z,\lambda}(r,z) = -\frac{\partial}{\partial z}U_\lambda(r,z) = -2\pi G\alpha\rho \int_0^\infty \frac{J_0(kr)\,\mathrm{d}k}{\sqrt{k^2+1/\lambda^2}}[bJ_1(kb) - aJ_1(ka)] \times \left[\mathrm{e}^{-\sqrt{k^2+1/\lambda^2}(z-\ell)} - \mathrm{e}^{-\sqrt{k^2+1/\lambda^2}(z+\ell)}\right] \tag{18}$$

$$F_{z,\lambda}(r,z) = -\frac{\partial}{\partial z}U_\lambda(r,z) = -2\pi G\alpha\rho \int_0^\infty \frac{J_0(kr)\,\mathrm{d}k}{\sqrt{k^2+1/\lambda^2}}[bJ_1(kb) - aJ_1(ka)] \times \left[\mathrm{e}^{-\sqrt{k^2+1/\lambda^2}(\ell-z)} - \mathrm{e}^{-\sqrt{k^2+1/\lambda^2}(\ell+z)}\right]. \tag{19}$$

In a similar fashion the radial force can be found from the first derivative of equations (16) and (17):

If $z \leqslant -\ell$ or $z \geqslant \ell$ then

$$F_{r,\lambda}(r,z) = -\frac{\partial}{\partial r}U_\lambda(r,z) = -2\pi G\alpha\rho \int_0^\infty \frac{J_1(kr)k\,\mathrm{d}k}{k^2+1/\lambda^2}[bJ_1(kb) - aJ_1(ka)] \times \left[\mathrm{e}^{-\sqrt{k^2+1/\lambda^2}(z-\ell)} - \mathrm{e}^{-\sqrt{k^2+1/\lambda^2}(z+\ell)}\right] \tag{20}$$

and if $-\ell \leqslant z \leqslant \ell$ then

$$F_{r,\lambda}(r,z) = -\frac{\partial}{\partial r}U_\lambda(r,z) = -2\pi G\alpha\rho \int_0^\infty \frac{J_1(kr)k\,\mathrm{d}k}{k^2+1/\lambda^2}[bJ_1(kb) - aJ_1(ka)] \times \left[2 - \mathrm{e}^{-\sqrt{k^2+1/\lambda^2}(\ell-z)} - \mathrm{e}^{-\sqrt{k^2+1/\lambda^2}(\ell+z)}\right]. \tag{21}$$

In particular, if the unit mass is considered to be placed on the z axis, then the *axial* force is

$$F_{z,\lambda}(0,z) = -2\pi G\alpha\rho \int_0^\infty \frac{\mathrm{d}k}{\sqrt{k^2+1/\lambda^2}}[bJ_1(kb) - aJ_1(ka)] \times \left[\mathrm{e}^{-\sqrt{k^2+1/\lambda^2}(z-\ell)} - \mathrm{e}^{-\sqrt{k^2+1/\lambda^2}(z+\ell)}\right] \tag{22}$$

for $z \leqslant -\ell$ or $z \geqslant \ell$ and

$$F_{z,\lambda}(0,z) = -2\pi G\alpha\rho \int_0^\infty \frac{\mathrm{d}k}{\sqrt{k^2+1/\lambda^2}}[bJ_1(kb) - aJ_1(ka)] \times \left[\mathrm{e}^{-\sqrt{k^2+1/\lambda^2}(\ell-z)} - \mathrm{e}^{-\sqrt{k^2+1/\lambda^2}(\ell+z)}\right] \tag{23}$$

for $-\ell \leqslant z \leqslant \ell$, respectively.

Equations (22) and (23) can be simplified by using one general formula (Prudnikov *et al* 1986):

$$\int_0^\infty \left(1/\lambda^2 + k^2\right)^{-1/2} \mathrm{e}^{-c\left(\frac{1}{\lambda^2}+k^2\right)} J_1(\gamma k)\,\mathrm{d}k = I_{1/2}\left(\frac{1}{2\lambda}[(c^2+\gamma^2) - c]\right) K_{1/2}\left(\frac{1}{2\lambda}[(c^2+\gamma^2) + c]\right).$$

Where $c = z \pm \ell$ or $c = \ell \pm z$, $\gamma = a$ or $\gamma = b$ and

$$I_{1/2}(z) = \frac{1}{\sqrt{2\pi z}}(\mathrm{e}^z - \mathrm{e}^{-z}) \qquad K_{1/2}(z) = \sqrt{\frac{\pi}{2z}}\mathrm{e}^{-z}.$$

One then easily obtains

$$F_{z,\lambda}(0,z) = -2\pi G\alpha\rho\lambda\left[\mathrm{e}^{-\frac{\sqrt{b^2+(z+\ell)^2}}{\lambda}} - \mathrm{e}^{-\frac{\sqrt{b^2-(z+\ell)^2}}{\lambda}} - \mathrm{e}^{-\frac{\sqrt{a^2+(z+\ell)^2}}{\lambda}} + \mathrm{e}^{-\frac{\sqrt{a^2+(z-\ell)^2}}{\lambda}}\right] \tag{24}$$

for both cases.

One particular case of equation (21) is for the infinitely long cylinder. Because the force does not depend on z, we find the radial force for the case $z = 0$:

$$F_r(r) = 4\pi G\alpha\rho\int_0^\infty \frac{J_1(kr)k\,\mathrm{d}k}{(k^2+1/\lambda^2)}[bJ_1(kb) - aJ_1(ka)]\int_0^\infty \mathrm{e}^{-\sqrt{k^2+1/\lambda^2}z'}\,\mathrm{d}z. \tag{25}$$

But from the integration formula (Prudnikov *et al* 1986)

$$\int_0^\infty \frac{k\,\mathrm{d}k}{k^2+1/\lambda^2}J_1(kr)J_1(kc) = I_1(c/\lambda)K_1(r/\lambda)$$

where $I_1(x)$ and $K_1(x)$ are modified Bessel functions, and $c = a$, or $c = b$ in this case. Equation (25) then becomes

$$F_r(r) = 4\pi G\alpha\rho[bI_1(r/\lambda)K_1(b/\lambda) - aI_1(r/\lambda)K_1(a/\lambda)]. \tag{26}$$

If we replace the unit mass by a uniform sphere having a total mass M_{sph}, and a radius R_{sph}, with its centre of mass placed at the point (r, φ, z), then all the expressions above for the unit point mass remain valid, but become multiplied by a factor $\xi_\lambda M_{\mathrm{sph}}$. The sphere's form-factor ξ_λ is (Gibbons and Whiting *et al* 1981)

$$\xi_\lambda = 3\left(\frac{\lambda}{R_{\mathrm{sph}}}\right)^3 \cdot \left[\frac{R_{\mathrm{sph}}}{\lambda}\cosh\left(\frac{R_{\mathrm{sph}}}{\lambda}\right) - \sinh\left(\frac{R_{\mathrm{sph}}}{\lambda}\right)\right]$$

which easily can be verified by direct integration of equation (2) over the body of sphere.

If, on the other hand, the unit mass were to be replaced by another cylindrical body, then equation (19) can be integrated straightforwardly over the test mass volume. Indeed this situation corresponds to the real experimental design that was proposed originally in the framework of the 'M2' STEP programme, in order to test Newton's inverse square law at the relatively short distance of a few centimetres (ESA SCI (93) 1993).

Considering now the situation in which a cylindrical test mass is placed (for example) inside an attracting mass that possesses the same symmetry, then one finds the axial forces between them to be

$$\begin{aligned} F_{z,\lambda}(r,z) = -2\pi G\alpha\rho\rho_s\int_0^\infty \frac{\mathrm{d}k}{k(k^2+1/\lambda^2)}[bJ_1(kb) - aJ_1(ka)][b_sJ_1(kb_s) - a_sJ_1(ka_s)] \\ \times\left[2 - \mathrm{e}^{-\sqrt{k^2+1/\lambda^2}(\ell+\ell_s-d)} - \mathrm{e}^{-\sqrt{k^2+1/\lambda^2}(\ell-\ell_s+d)}\right. \\ \left. - \mathrm{e}^{-\sqrt{k^2+1/\lambda^2}(d+\ell_s-\ell)} + \mathrm{e}^{-\sqrt{k^2+1/\lambda^2}(\ell+\ell_s+z)}\right] \end{aligned}$$

where a_s, b_s and ℓ_s are the inner and outer radii, and semi-length of the test mass respectively, and d is the distance between the cylinders' centres of mass.

Similar formulae exist to those of equations (18)–(21) for both the cases of a cylindrical test mass placed inside or outside a cylindrical attracting mass. Thus, in general, the usually required 6D integration of the gravitational interaction—carried out over the volumes of two cylindrical bodies—can be replaced by the 1D infinite-range integration above. Furthermore this infinite-range integration can be replaced by a finite integration (see appendix).

4. Analysis of the experimental tests of the inverse square law of gravitation

The most sensitive and accurate methods used to verify the inverse square law are the Cavendish-type laboratory measurements. The physical basis of such experiments consists in the measurement of the dynamical parameters of a high-quality torsion balance, placed in the gravitational field produced by source masses of well defined shape and density. Typical distances at which the source and test masses can be separated are from about 1 to 10^3 cm. The limited scale of the laboratory gravity experiments is a consequence of the extreme weakness of the gravitational interaction.

The first result indicating a violation of the inverse square law was reported by Long (1976). He claimed that the inverse square law of gravity breaks down at the distance scale of the order of 0.1 m. This stimulated a great deal of subsequent experiment work, and, for example, Spero *et al* (1980) carried out an experimental test of the inverse square law. His results were in obvious conflict with those of Long. In the α–λ plot, interpreted within the framework of a single Yukawa potential term, then Long's data are in the area of Spero *et al*'s 'excluded' part. Subsequently all other experiments, Hoskins *et al* (1985) and Chen *et al* (1984) etc, find negative results, as shown in figure 1.

Figure 1 is interpreted by assuming the masses are point masses, for one Yukawa force term. However, there is a strong suggestion that such terms should be associated in pairs with opposite sign. That is, an attractive force would be accompanied by a repulsive one to give near cancellation. If one, then why not two?—indeed the result for one Yukawa term may be quite different from that using two terms, e.g. Stacey *et al* (1987), Fischbach *et al* (1991).

In the following we shall use the fully analytical formulae developed above to treat the 3D cylindrical bodies that were used in both Long's and Spero *et al*'s experiments, and then reanalyse their results in this light for both one and two Yukawa force terms.

4.1. Long's experiment

The principle of the experiment performed by Long (1976), shown in figure 3, is that the dimensions and masses of the two rings, one large and one small, are chosen so that the maximum force exerted by each is the same—according to the inverse square law. The far ring (the larger one) was made of brass, and weighed 57 580.83 g. It was 7.633 cm thick from back to front, and the inner and outer radii were 21.589 cm and 27.112 cm, respectively. The near ring (the smaller of the two) was made of tantalum, and weighed 1255.271 g. Its thickness was 1.7765 cm, and its inner and outer radii were 2.7513 cm and 4.5536 cm, respectively. As the Newtonian field of the rings is very flat at the 'Helmholtz' point, the positional accuracy in the placement of the rings was considered not to be so great.

The *Newtonian* force of a ring along its cylindrical axis is

$$F_z = 2\pi G\rho \left\{ \sqrt{a^2 + (z-\ell)^2} - \sqrt{a^2 + (z+\ell)^2} - \sqrt{b^2 + (z-\ell)^2} + \sqrt{b^2 + (z+\ell)^2} \right\} \quad (27)$$

where a and b are the inner and outer radii, respectively, and ℓ is semi-length (semi-thickness) of the ring.

From setting $\frac{\partial F_z}{\partial z} = 0$ we find the ring locations to be $Z_{\max} = 17.415$ (cm) for the large ring and $Z_{\max} = 2.6088$ (cm) for the small ring. These values are consistent with those of Long, although in his paper the indicated distances seem to be measured from the surface of the rings, instead of from their centres.

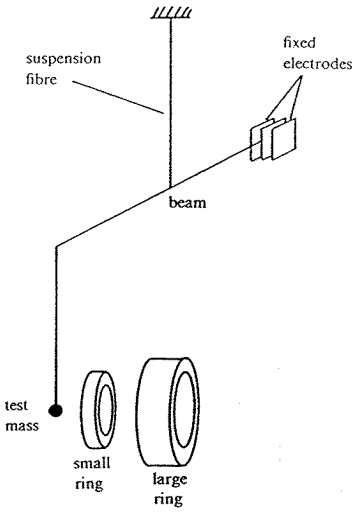

Figure 3. Apparatus used in Long's experiment (1976)—see text for details.

The gravitational force was detected with a 48.6 cm Cavendish torsion balance, and the test mass was a sphere of tantalum weighing 50 g which was suspended 87 cm below the arm of the balance.

Long expressed his results in terms of the relative difference of torque produced by the rings. If T_ℓ is the torque exerted by the large ring and T_s that exerted by the small ring, then their relative difference is equal to

$$\Delta = \frac{T_\ell - T_s}{T_s}. \tag{28}$$

When the departures from the nominal dimensions and masses of the rings are taken into account, and the forces of the rings on the balance-arm are taken into account, the relative difference of torque for Newtonian gravity would be $\Delta_N = 0.03807 \pm 0.0005$. The experimental value, Δ, was found by measuring directly the torque difference $T_\ell - T_s$, by first putting one ring and then the other in position. This gave a value of $\Delta = 0.04174 \pm 0.0004$.

If $F_{\ell,N}$, $F_{l,NN}$ and $F_{s,N}$, $F_{s,NN}$ are Newtonian and non-Newtonian forces for the large and small rings, respectively, then

$$\Delta = \frac{T_\ell - T_s}{T_s} = \frac{(F_{\ell,N} + F_{\ell,NN}) - (F_{s,N} + F_{s,NN})}{(F_{s,N} + F_{s,NN})}$$
$$= \frac{F_{\ell,N} - F_{s,N}}{(F_{s,N} + F_{s,NN})} + \frac{F_{\ell,NN} - F_{s,NN}}{(F_{s,N} + F_{s,NN})}.$$

As $F_{\ell,NN}$ and $F_{s,NN}$ are proportional to α and much smaller than $F_{s,N}$, and if the second and higher powers of α are ignored, then

$$\Delta = \frac{F_{\ell,N} - F_{s,N}}{F_{s,N}}\left(1 - \frac{F_{s,NN}}{F_{s,N}}\right) + \frac{F_{\ell,NN} - F_{s,NN}}{F_{s,N}}$$
$$= \Delta_N\left(1 - \frac{F_{s,NN}}{F_{s,N}}\right) + \Delta_{NN} \tag{29}$$

where $\Delta_{NN} = (F_{\ell,NN} - F_{s,NN})/F_{s,N}$, and $F_{\ell,NN}$ and $F_{s,NN}$ can be calculated using the formulae above (equations (24) and (29)).

4.2. The experiments of Spero et al (1980)

Spero *et al* (1980) carried out an experiment based on an analogue of the Faraday cage in electromagnetism, as shown in figure 4. They used a torsion balance to measure the change in the force acting on a test mass suspended inside a long hollow cylinder, as the cylinder was moved laterally. If the inverse square law holds, then the force inside an infinitely long cylinder should be zero. Because it is not possible to make an infinitely long cylinder, and as the test mass of a torsion balance has to be placed inside it, Spero *et al* used a cylinder of length $L = 60$ (cm) and inside diameter $D = 6$ (cm). There exists a small net 'end-effect', but this need not be taken into account. The cylinder, of mass 10.44 kg and wall thickness 1 cm, was made of high-purity double-vacuum-melted, type-316 stainless steel. The test mass was a 20 g, 4.4 cm long cylinder of copper, hanging 83 cm below the end of a torsion-balance boom of total length 60 cm.

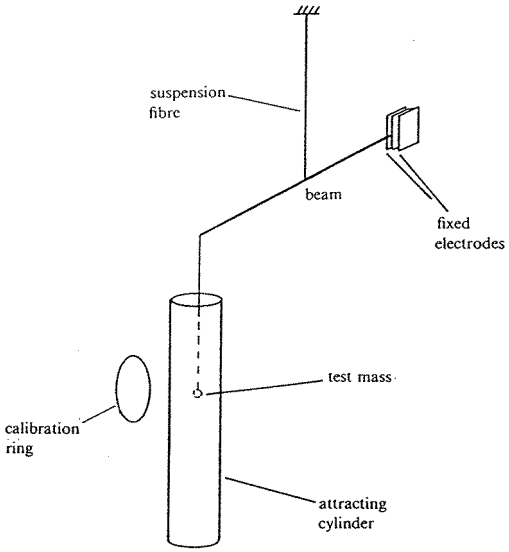

Figure 4. Apparatus used in Spero *et al*'s experiment (1980)—see text for details.

Spero *et al* presented their results as the torque change $\Delta\Gamma$ on the balance, as the cylinder moved through a cycle. After comparing the total Newtonian predicted $\Delta\Gamma$ with the experimental value they found

$$\begin{aligned}\delta &= \Delta\Gamma(\text{expt.}) - \Delta\Gamma(\text{theor.}) \\ &= (0.02 \pm 0.14) \times 10^{-13}\ \text{N m}^{-1} \cdots (\times 10^{-6}\ \text{dyn cm}^{-1}).\end{aligned} \tag{30}$$

δ can be evaluated by using formulae above, as $\delta = 2F_{\text{NN}}d$, where d is the arm length of the torsion balance (equations (26) and (30)).

4.3. Interpretation of the experimental results using two Yukawa terms

The non-Newtonian potential with two Yukawa terms can be written as

$$V_{\text{NN}} = \alpha\frac{\text{e}^{-r/\lambda_\alpha}}{r} - \beta\frac{\text{e}^{-r/\lambda_\beta}}{r}$$

the case of just one term being simulated by setting $\beta = 0$. The force corresponding to the above potential can be written as $F_{\text{NN}} = (\alpha f_{\alpha,\text{NN}} - \beta f_{\beta,\text{NN}})\rho$, where $f_{\alpha,\text{NN}}$ and $f_{\beta,\text{NN}}$ correspond to the Yukawa type force described above in slightly different form, for the

convenience of analysis. Equation (24) is the axial force due to the non-Newtonian term for an interaction between a cylindrical body and a point test mass, and so it can be used directly for analysis of Long's experiment. Similarly, equation (26) can be used directly for analysis of Spero *et al*'s experiment.

Inserting Long's experimental data into equation (24), and by using equation (29), one obtains constraint equations for the α and λ of Long's experiment (considering firstly only one Yukawa term). The allowed region for α and λ can be calculated by using this constraint equation, whilst varying the parameter λ. Inserting Spero *et al* 's experimental data into equations (26) and (30), one can find the allowed region of α and λ for this experiment as well. The interpreted results are plotted in figure 5.

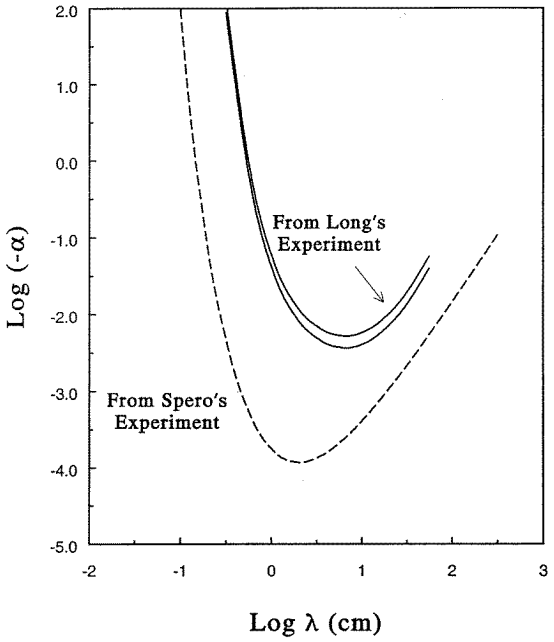

Figure 5. Broken curve: the analysis of this work, showing the calculated limit to the allowed values for the parameters α and λ, using a single Yukawa term. Excluded α–λ values lie above the broken curve.

A similar calculation can be carried out for two Yukawa terms. Here two special cases are considered. One is for the ratio $R_{ab} = \beta/\alpha = 0.99$—making the two terms nearly cancel each other out, and the other is for $R_{ab} = 0.09$—making one term dominate over the other, in both cases for the specific condition $\lambda_\alpha = \lambda_\beta$. These results are plotted in figure 6.

Figures 5 and 6 show clearly that the α–λ graph for two Yukawa terms has a similar behaviour to the α–λ graph when only a single Yukawa term is considered, and indeed Long's results are found to be in the region which Spero *et al*'s exclude, for both situations. This means that the positive result of Long's experiment is still in conflict with that of Spero *et al*'s work, even under this more wide-ranging and detailed analysis. This is true for both one and two Yukawa terms. It is likely that the same results will be obtained for Chen's experiment, and others that are consistent with Spero *et al*'s result.

5. Conclusions

The analytical treatment of Yukawa type non-Newtonian forces in cylindrical geometry has been used for the reinterpretation of gravitational experiments searching for a 'fifth force'. This work starts from a very general form of Yukawa force, leading on to calculate analytic

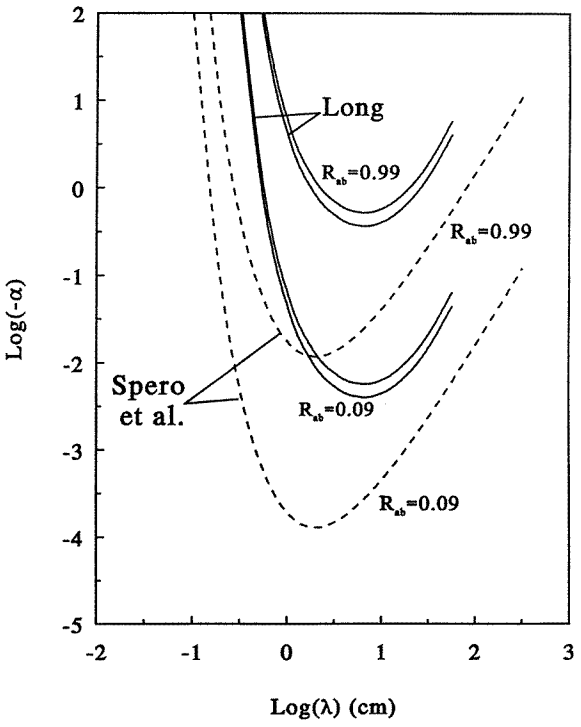

Figure 6. Broken curves: the analysis of this work, showing the calculated limits to the allowed values for the parameters α and λ, modelled using two Yukawa terms. The strengths of these two terms are denoted by α and β in the text, and the figure shows the analysis as carried out for two values of their relative strength $R_{ab} = \beta/\alpha$. Excluded α–λ values lie above the respective broken curves.

expressions for both axial and radial forces. The theory concerns the interaction between a point gravitational source and a cylindrical body, and between two cylindrical bodies, as well as between a point source and a sphere. The considerations here have been general and can be widely applied to other fifth force experiments.

Two practical examples of their application have been to use them for reanalysis of the results of Long's and Spero's experiments. Although the results support those of other work, this work provides further meaningful support to the Newtonian gravitational inverse square law of gravitation. It also gives a demonstration of the validity of the methods developed above.

Appendix. On evaluation of some integrals involving the Bessel functions

In this appendix, we will show that the infinite integration in equation (A1) below can be replaced by a finite integration. We begin by representing the previous formulae above (equations (18)–(23)) as a linear combination of the following type of infinite integral:

$$I^{(\alpha,\beta)}_{(\nu,\mu)}(p,q,s,\lambda) = \int_0^\infty \frac{\mathrm{d}k k^{1-\alpha}}{(k^2+1/\lambda^2)^{\beta/2}} J_\nu(kp) J_\mu(kq) \mathrm{e}^{-s\sqrt{k^2+1/\lambda^2}}. \tag{A1}$$

The authors of this paper have not found the explicit value of the integral above for any particular values of the parameters $(\alpha, \beta, \nu, \mu)$—even in the best collections of tabulated integrals. On the other hand, numerical evaluation of the infinite integrals is not convenient, due to the rapidly oscillating Bessel-function product under the integral sign.

First let us consider the following integral

$$I^{(2,1)}_{(1,1)}(p,q,s,\lambda) = \int_0^\infty \frac{\mathrm{d}k}{k(k^2+1/\lambda^2)^{1/2}} J_1(kp) J_1(kq) \mathrm{e}^{-s\sqrt{k^2+1/\lambda^2}} \tag{A2}$$

where p, q and s are arbitrary positive parameters. Consider the expressions

$$\frac{J_1(kp)J_1(kq)}{k} = f(k) = \int_0^\infty J_1(kt)f(t)t\,\mathrm{d}t$$
$$f(t) = \int_0^\infty J_1(kt)f(k)k\,\mathrm{d}k = \int_0^\infty J_1(kt)J_1(kp)J_1(kq)\,\mathrm{d}k. \tag{A3}$$

The value of equation (A3) differs from zero only if the values of the parameters p, q, t can form a triangle as shown in the following figure.

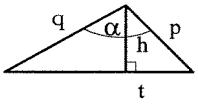

It means that the value of the image function $f(t)$ in equation (A3) is equal to zero for all values of the parameter t, except for the situation $|p-q| < t < p+q$, in which case $f(t)$ can be represented in the following way:

$$f(t) = \frac{2\Delta(p,q,t)}{\pi tpq} = \frac{h(p,q,t)}{\pi pq} \tag{A4}$$

where $\Delta(p,q,t)$ and $h(p,q,t)$ are the area of the triangle and its height, respectively. It is straightforward to show that

$$I^{(2,1)}_{(1,1)}(p,q,s,t) = \frac{1}{\pi pq}\int_{|p-q|}^{p+q} h(p,q,t)t\,\mathrm{d}t \int_0^\infty \frac{\mathrm{d}k}{\sqrt{k^2+1/\lambda^2}} J_1(kt)\mathrm{e}^{-s\sqrt{k^2+1/\lambda^2}}$$
$$= \frac{\lambda}{\pi pq}\int_{|p-q|}^{p+q} h(p,q,t)\,\mathrm{d}t\left(\mathrm{e}^{-s/\lambda} - \mathrm{e}^{-\sqrt{s^2+t^2}/\lambda}\right). \tag{A5}$$

We can change the variable of integration to avoid the arbitrary parameters from the integration limits. Taking account of the following obvious relations

$$h = \frac{pq\sin\alpha}{\sqrt{p^2+q^2-2pq\cos\alpha}}$$
$$t = \sqrt{p^2+q^2-2pq\cos\alpha}$$
$$dt = \frac{pq\sin\alpha\,\mathrm{d}\alpha}{\sqrt{p^2+q^2-2pq\cos\alpha}}$$

we have, finally:

$$I^{(2,1)}_{(1,1)}(p,q,s,\lambda) = \frac{\lambda}{\pi}pq\int_0^\pi \frac{\sin^2\alpha\,\mathrm{d}\alpha}{p^2+q^2-2pq\cos\alpha}\left(\mathrm{e}^{-s/\lambda} - \mathrm{e}^{-\sqrt{s^2+p^2+q^2-2pq\cos\alpha}/\lambda}\right). \tag{A6}$$

Using similar arguments it is straightforward to show that

$$I^{(2,0)}_{(1,1)}(p,q,s,\lambda) = \frac{1}{\pi}pq\int_0^\pi \frac{\sin^2\alpha\,\mathrm{d}\alpha}{p^2+q^2-2pq\cos\alpha}$$
$$\times\left(\mathrm{e}^{-s/\lambda} - \frac{s}{\sqrt{s^2+p^2+q^2-2pq\cos\alpha}}\mathrm{e}^{-\sqrt{s^2+p^2+q^2-2pq\cos\alpha}/\lambda}\right) \tag{A7}$$

and

$$I^{(0,1)}_{(1,1)}(p,q,s,\lambda) = \frac{1}{\pi}pq\int_0^\pi \frac{\sin^2\alpha\,\mathrm{d}\alpha}{s^2+p^2+q^2-2pq\cos\alpha}$$
$$\times\left(\frac{1}{\lambda} + \frac{1}{\sqrt{s^2+p^2+q^2-2pq\cos\alpha}}\right)\mathrm{e}^{-\sqrt{s^2+p^2+q^2-2pq\cos\alpha}/\lambda}. \tag{A8}$$

Other forms of the integrals represented by equation (A1) can be related to equations (A6)–(A8). For example, it is straightforward to check that

$$I^{(1,1)}_{(0,1)}(p,q,s,\lambda) \equiv \frac{1}{p}\frac{\partial}{\partial p}(pI^{(2,1)}_{(1,1)}(p,q,s,\lambda)) \tag{A9}$$

$$I^{(0,2)}_{(1,1)}(p,q,s,\lambda) = \int_s^\infty I^{(0,1)}_{(1,1)}(p,q,x,\lambda)\,\mathrm{d}x \tag{A10}$$

$$I^{(2,2)}_{(1,1)}(p,q,s,\lambda) = \lambda^2[I^{(2,0)}_{(1,1)}(p,q,s,\lambda) - I^{(0,2)}_{(1,1)}(p,q,s,\lambda)]. \tag{A11}$$

References

Fischbach E and Talmadge C 1992 Six years of the fifth force *Nature* **356** 207

Chen Y T and Cook A 1993 *Gravitational Experiments in the Laboratory* (Cambridge: Cambridge University Press)

Lockerbie N A, Veryaskin A V and Xu X 1993 Differential gravitational coupling between cylindrical-symmetric, concentric test masses and an arbitrary gravitational source: relevance to the STEP experiment *Class. Quantum Grav.* **10** 2419–30

Lockerbie N A, Xu X and Veryaskin A V 1994 Optimization of immunity to helium tidal influences for the STEP experiment test-masses *Class. Quantum Grav.* **11** 1975–90

Prudnikov A P, Brychkov Yu A and Marichev O I 1986 *Integrals and Series* vols 1 and 2 (Oxford: Gordon and Breach)

Gibbons G W and Whiting B F 1981 Newtonian gravity measurements impose constraints on unification theories *Nature* **291** 636

ESA SCI (93) 4 March 1993 STEP Satellite Test of the Equivalence Principle, Report on the Phase A Study

Cook A 1988 Experiment on gravitation *Rep. Prog. Phys.* **51** 707–57

Hawking S W and Israel W (eds) 1987 *300 Years of Gravitation* (Cambridge: Cambridge University Press)

Hoskins J K, Newman R D, Spero R and Schultz J 1985 Experimental tests of the gravitational inverse-square law for mass separations from 2 to 105 cm *Phys. Rev.* D **32** 3084

Goodkind J M, Czipott P V, Mills A P Jr, Murakami M, Platzman P M, Young C W and Zuckerman D M 1993 Test of the gravitational inverse-square law at 0.4- to 1.4-m mass separations *Phys. Rev.* D **47** 1290

Chan H A, Moody M V and Paik H J 1982 Null test of the gravitational inverse-square law *Phys. Rev. Lett.* **49** 1745

Chen Y T, Cook A H, FRS and Metherell A J F 1984 An experimental test of the inverse square law of gravitation at range of 0.1 m *Proc. R. Soc.* A **394** 47–68

Stacey F D, Tuck G J and Moore G I 1987 Quantum gravity: Observational constraints on a pair of Yukawa terms *Phys. Rev.* D **36** 2374

Fischbach E, Talmadge C and Krause D 1991 *Phys. Rev.* D **43** 460

Long D R 1976 *Nature* **260** 417

Spero R, Hoskins J K, Newman R, Pellam J and Schultz J 1980 Test of the gravitational inverse square law at laboratory distances *Phys. Rev. Lett.* **44** 1645